As originally published in the IPC APEX EXPO Conference Proceedings.

Long Term Reliability Analysis of Lead Free and Halogen Free Electronic Assemblies

Gregory Morose, Sc.D., Toxics Use Reduction Institute (TURI), Lowell, MA
Sammy Shina, Ph.D., University of Massachusetts, Lowell, MA
Bob Farrell and Paul Bodmer, Benchmark Electronics, Hudson, NH
Ken Degan, Teradyne Inc., North Reading, MA
David Pinsky, Karen Ebner, and Amit Sarkhel,
Raytheon Company, Tewksbury, MA
Richard Anderson Ph.D., and Helena Pasquito, Cobham, Lowell, MA
Michael Miller and Louis Feinstein, Textron Systems, Wilmington, MA
Deb Fragoza, Eric Ren, EMC, Hopkinton, MA
Roger Benson, Carsem, Attleboro, MA
Charlie Bickford, Wall Industries, Exeter, New Hampshire

Abstract
The New England Lead Free Consortium, composed of many companies in the electronic supply chain in the regional area and chaired by the author; has embarked on an extensive long term reliability study of lead-free and halogen free electronic assemblies. Specialized PCB's were built, assembled and reworked at the consortium member companies using multiple types of laminates, PCB surface finishes and various component types including through-hole and surface mount technology. The assemblies were examined for visual characteristics and subsequently tested for reliability using temperature cycling as well as vibration testing. All rework, reliability tests, and evaluations have used or will be using industry standards, methods and techniques for easy reference to other long term reliability studies. The studies will include comparison to a baseline of leaded electronic assemblies. This paper will outline results obtained so far into the long term reliability study.

Introduction
For the past decade, there has been a global effort in the electronics industry to initiate a move towards using lead-free materials for the production of printed circuit boards. However, there are numerous technical challenges, such as long term reliability and rework capability, which remain to hinder the universal implementation of lead-free materials. Consequently, many electronics products are still currently manufactured and assembled using materials containing lead.

This research included an evaluation of the assembly of test vehicles using various lead-free, halogen-free and nano-materials. The test vehicles included a variety of both surface mount and through hole components. The lead-free materials evaluated during the assembly included various component finishes, four board surface finishes, two laminate materials, three through hole component solders, and four surface mount component solder pastes. These test vehicles were then subjected to thermal cycling to evaluate the long term reliability of these assemblies. The results of the lead-free assemblies were compared against baseline data obtained by assembling test vehicles with tin/lead materials. In addition, research was conducted on the effectiveness of lead-free materials for rework capability of through hole components. Vibration testing will be conducted in the future.

This research was conducted by the New England Lead-free Electronics Consortium, which is a collaborative effort of New England companies spanning the electronics supply chain to help move the industry towards lead-free electronics. This consortium has been sponsored and supported by the Toxics Use Reduction Institute (TURI), the U.S. Environmental Protection Agency (EPA), and the University of Massachusetts Lowell. For the past several years, this consortium has conducted research and testing for using various lead-free materials for the assembly of printed circuit boards.

Methodology
The technique of Design of Experiments (DoE) was used to separate the effect of each parameter on the overall performance of quality and reliability of the test vehicles. The test parameters were as follows:
1. **Components.** There were 886 SMT components (BGAs, microBGAs, resistors, TSOPs, PQFPs, PQFN, and MLFs), and 21 THT components (connectors, LEDs, DC/DC convertors, and capacitors) provided for assembly of each test vehicle.
2. **Solder types.** There were 24 test vehicles that were assembled with lead free materials and solders, 8 test vehicles that were assembled with leaded solder, and three halogen free test vehicles that were assembled with lead free solders.

3. **PWB finishes**. There were four types of surface finishes:
   - Electroless Nickel Immersion Gold (ENIG).
   - Hot Air Solder Leveling (HASL). A tin/copper alloy was used. It is comprised of mostly tin, but also includes 0.6% copper, 0.05% nickel, and 0.0055% germanium.
   - Organic Solderability Preservatives (OSP).
   - Nano surface finish using nanosilver particles dispersed in a polymer (polyaniline), with a thickness between 45 to 65 nm. This was selected because it has the potential of addressing major lead free implementation challenges such as copper dissolution during rework and process improvement for assembly of lead free THT components.
4. **Solders**. There were four different solder pastes used for assembly of the SMT components:
   - Tin/silver/copper alloy (SAC305) with no clean chemistry flux (from two different suppliers).
   - Tin/silver/copper alloy (SAC305) with organic acid chemistry flux.
   - Tin lead alloy with no clean chemistry flux for baseline data source.

   Three (3) different solder alloys were used in for the assembly of the THT components:
   - Tin/silver/copper alloy (SAC305).
   - Tin/copper alloy at two different operational settings, 295 and 310 ^{o}C solder pot temperatures
   - Tin/lead alloy for baseline purposes.
5. **Laminates**. Two different laminate materials were used:
   - FR-4 laminate material was designed for use in lead free assembly environments (32 test vehicles in the DoE) and has a glass transition (T_g) temperature of 180°C.
   - Halogen-free laminate with a glass transition (T_g) temperature of 180°C was used for three (3) test vehicles outside of the DoE.

6. **Test Vehicle**. Thirty five (35) test vehicles were assembled for this research and a photograph of an assembled test vehicle is shown in Figure 1. The test vehicles were 8" (inches) wide by 10" long, contained 20 layers, and were 0.110" thick.

Figure 1: Assembled Test Vehicle

7. **Experiment Matrices**: These matrices are based on DoE principles and were used to selectively determine the individual contribution of each parameter. They are shown in the following Tables 1, 2 and 3 for the 35 test vehicles. The lead-free test vehicles are shown in Table 1.

Table 1: **Lead free Test Vehicles in DoE**

Test Vehicle	SMT Solder	TH Solder	Surface Finish	Laminate
1	SAC305 - 1	SAC305	ENIG	FR4
2	SAC305 - 1	SAC305	ENIG	FR4
3	SAC305 - 1	SAC305	HASL	FR4
4	SAC305 - 1	SAC305	HASL	FR4
5	SAC305 - 1	SAC305	OSP	FR4
6	SAC305 -1	SAC305	OSP	FR4
7	SAC305 - 1	SAC305	Nano	FR4
8	SAC305 - 1	SAC305	Nano	FR4
9	SAC305OA	Tin/copper 1	ENIG	FR4
10	SAC305OA	Tin/copper 1	ENIG	FR4
11	SAC305OA	Tin/copper 1	HASL	FR4
12	SAC305OA	Tin/copper 1	HASL	FR4
13	SAC305OA	Tin/copper 1	OSP	FR4
14	SAC305OA	Tin/copper 1	OSP	FR4
15	SAC305OA	Tin/copper 1	Nano	FR4
16	SAC305OA	Tin/copper 1	Nano	FR4
17	SAC305- 2	Tin/copper 2	ENIG	FR4
18	SAC305- 2	Tin/copper 2	ENIG	FR4
19	SAC305- 2	Tin/copper 2	HASL	FR4
20	SAC305- 2	Tin/copper 2	HASL	FR4
21	SAC305- 2	Tin/copper 2	OSP	FR4
22	SAC305- 2	Tin/copper 2	OSP	FR4
23	SAC305- 2	Tin/copper 2	Nano	FR4
24	SAC305- 2	Tin/copper 2	Nano	FR4

The DoE experiments were full factorial, except when examining the effects of the halogen free laminates, given that the consortium was limited in resources. It was decided to use t-tests for comparison of this parameter. The baseline leaded test vehicles are shown in Table 2.

Table 2: **Tin Lead Test Vehicles in DoE**

Test Vehicle	SMT Solder	TH Solder	Surface Finish	Laminate
25	Tin Lead	Tin Lead	ENIG	FR4
26	Tin Lead	Tin Lead	ENIG	FR4
27	Tin Lead	Tin Lead	HASL	FR4
28	Tin Lead	Tin Lead	HASL	FR4
29	Tin Lead	Tin Lead	OSP	FR4
30	Tin Lead	Tin Lead	OSP	FR4
31	Tin Lead	Tin Lead	Nano	FR4
32	Tin Lead	Tin Lead	Nano	FR4

All three (3) halogen free test vehicles were made with OSP laminate finish, as shown in Table 3. All three were soldered with SAC305 solder paste, two with no-clean flux and one with organic acid flux. The halogen free laminates were made with FR4 laminate with a 180 ^{o}C Tg, and are shown in Table 3.

Table 3: **Halogen free Test Vehicles**

Test Vehicle	SMT Solder	TH Solder	Surface Finish	Laminate
33	SAC305-NC1	SAC305	OSP	HF
34	SAC305-NC1	SAC305	OSP	HF
35	SAC305OA	SAC305	OSP	HF

The even numbered test vehicles were included in the thermal cycling efforts, and the odd-numbered test vehicles will be included in the future vibration testing.

Rework

The through-hole component used for the through hole rework process was the Samtec 200 pin connector (Part Number: YTQ-150-03-L-Q). The pin dimensions for this component are 0.020 inches square, and the pin finish is matte tin. This component was selected because it would be a challenge to successfully rework this component given the thickness of the rework coupon (0.110 inches). The figure below shows the Samtec 200 pin through hole connector mounted on the upper left hand corner at component location J5 of the rework coupon.

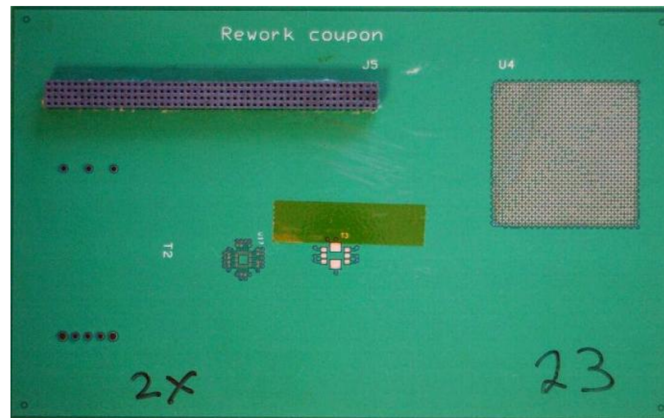

Figure 2: Rework Coupon with Through Hole Connector

The through hole component rework process included the following four surface finishes: OSP, ENIG, lead-free HASL (using the tin/copper alloy), and nano. The through hole rework process included only one llaminate material: High Tg FR4. Because of time and resource constraints, the halogen-free laminate material was not included in these efforts. Two different lead-free solder alloys were used for this experiment: SAC 305 solder and tin/copper solder. In addition, there were three different rework processes used that are described in further detail later in this section. There were twenty-four rework coupons included in the through hole component single rework effort. This provided a balanced Design of Experiments for the single rework efforts. The Design of Experiments is shown in the table below.

Table 1: Single Rework Design of Experiments

Coupon Number	Solder	Process	Surface Finish
1	SAC305	1	ENIG
2	SAC305	1	HASL
3	SAC305	1	Nano
4	SAC305	1	OSP
5	SAC305	2	ENIG
6	SAC305	2	HASL
7	SAC305	2	Nano
8	SAC305	2	OSP
9	SAC305	3	ENIG
10	SAC305	3	HASL
11	SAC305	3	Nano
12	SAC305	3	OSP
13	Tin/copper	1	ENIG
14	Tin/copper	1	HASL
15	Tin/copper	1	Nano
16	Tin/copper	1	OSP
17	Tin/copper	2	ENIG
18	Tin/copper	2	HASL
19	Tin/copper	2	Nano
20	Tin/copper	2	OSP
21	Tin/copper	3	ENIG
22	Tin/copper	3	HASL
23	Tin/copper	3	Nano
24	Tin/copper	3	OSP

There were three different rework processes that were used for reworking the through hole components. For each of these processes, a board preheat temperature of 130 ^{o}C was used for the rework machine, and no clean flux was used at the component site. The solder pot temperature was 270 ^{o}C for the SAC 305 solder, and 287 ^{o}C for the tin/copper alloy. These three processes are described below:

Process 1: The Premier Rework RW116 machine was used for initial component installation, component removal, and second component installation. This process used a standard nozzle design.

Process 2: The Premier Rework RW116 machine was used for initial component installation, component removal and second component installation. This process used a hybrid nozzle design. The hybrid nozzle was a special proprietary design to address the challenges of copper dissolution during the rework process with lead-free solders. The intent of the design was to minimize solder flow at the surface of the test vehicle, but maintain adequate heat transfer to the solder so that there is not a significant drop in solder temperature during rework operations.

Process 3: The Premier Rework RW116 was used for the initial and second component installation. This process used the standard nozzle design for component installation. The Air Vac DRS25 was used for component removal.

Previous studies have found that forced convection for component removal together with solder fountain for component installation during rework can have an impact on decreasing copper dissolution rates. (Farrell, 2007)

The parameters for each of the steps for using the Air Vac machine for component removal are summarized in the table below.

Table 5: Air Vac Operation

Operation	**Rework Coupons with SAC305 Solder**	**Rework Coupons with Tin/copper Solder**
Preheat to 120 ^{o}C	Nozzle off	Nozzle off
Preheat to 160 ^{o}C	Nozzle on with 100% airflow	Nozzle on with 100% airflow
90 second ramp	Target temperature: 195 - 205 ^{o}C	Target temperature: 205 - 215 ^{o}C
80 second reflow	Target temperature: 225 - 235 ^{o}C	Target temperature: 235 – 245 ^{o}C
Remove component	Remove nozzle	Remove nozzle
Maintain coupon temperature	160 – 175 ^{o}C	160 – 175 ^{o}C
Vacuum solder from the connector holes	Target temperature: Greater than 221 ^{o}C	Target temperature: Greater than 227 ^{o}C

The key measurements made during the through hole rework process were contact time and copper dissolution. The contact time when the solder in the nozzle is in contact with the bottom surface of the rework coupon was measured for each step in the rework process. For Processes 1 and 2, this included contact time during initial component installation, component removal, and second component installation. For Process 3, this included contact time during initial component installation and second component installation.

Thermal Cycling

Each of the test vehicles had fourteen daisy chains to monitor solder joint integrity during the actual testing. The thermal cycling included sixteen test vehicles from the Design of Experiments. In addition, two test vehicles using the halogen-free laminate were also included, resulting in a total of eighteen test vehicles for the thermal cycling test.

The thermal cycling done for this research included an exception to the IPC-9701 standard: the dwell time at the temperature extremes was fifteen minutes instead of ten minutes for the thermal cycling. The IPC standard was developed to primarily address tin/lead solder materials. SAC solders have a lower creep rate than tin/lead solders at thermal cycle temperatures. This limits the amount of SAC solder damage during a short dwell time. Increasing the dwell time during thermal cycling for SAC solder has been reported to lead to a decreasing characteristic lifetime for typical thermal cycling conditions. (Manock, 2008) The intent of changing to a fifteen minute dwell time was to provide additional time to allow creep for the lead-free solders to reach completion. The monitoring for the thermal cycling was conducted by using an Agilent 34980A data logger.

The Agilent data logger is capable of scanning as many as 100 channels per second. Therefore, all 252 channels were able to be scanned in less than five seconds. This scanning rate satisfies the IPC 9701 requirement that the maximum scan interval for all daisy chains be one minute or less. Four of the fourteen daisy chains on the test vehicles are connected to discrete components (i.e. 0402, 0603, and 0805 resistors). Each of these daisy chains contains approximately 50 - 100 discrete components connected in series. Therefore, monitoring of these daisy chains only detected the first failure for each of the daisy chains on each of the test vehicles. Consequently, we were not able to determine when 63% failure occurs for discrete components.

The other ten daisy chains on the test vehicle are connected to only one component per daisy chain. The daisy chain is connected to each solder joint of the component. If one solder joint of the component fails, then the data logger detected a failure for that daisy chain. A complete listing of the daisy chain connections can be seen in the table below.

Table 6: Daisy Chain Connections on the Test Vehicle

Component RefDes	Component Type	Qty
R2 to R472	0402 Resistor, 0 ohm	100
R21 to R499	0603 Resistor, 0 ohm	100
R5 to R462	0805 Resistor, 0 ohm	49
R15 to R493	0805 Resistor, 0 ohm	52
U1	SMT, TSOP, 48 Pins	1
U2	SMT, TSOP, 48 Pins	1
U24	SMT, TSOP, 48 Pins	1
U25	SMT, TSOP, 48 Pins	1
U15	SMT, PQFP208	1
U14	SMT, Plastic BGA, 256 balls, 1.0 mm pitch	1
U18	SMT, Plastic BGA, 256 balls, 1.0 mm pitch	1
U16	SMT, Chip array BGA, 100 balls, 1.0 mm pitch	1
U17	SMT, Tape array uBGA, 64 balls, 0.5 mm pitch	1
U26	SMT, Ceramic u-BGA, 0.5mm pitch	1

Prior to thermal cycling, all assembled test vehicles received accelerated thermal aging consisting of a bake-out period of 24 hours at 100 ^{o}C. The thermal cycling was then initiated during June, 2008 at the Textron Systems facility in Wilmington, MA for approximately 1,000 cycles. The test vehicles and data logger were then moved to Cobham (M/A-COM) facility in Lowell, MA for additional thermal cycling. This report includes the results for 1,470 thermal cycles.

The parameters used for the thermal cycling included a high temperature of 125 ^{o}C and a low temperature of -55 ^{o}C, resulting in a total temperature differential of 180 ^{o}C between the high and low temperature extremes. These maximum and minimum temperatures are based upon IPC-9701, Test condition #4. The low temperature dwell time was fifteen minutes, and the high temperature dwell time was fifteen minutes. The temperature ramp rate was approximately 5 ^{o}C per minute. Therefore, the overall cycle time was 102 minutes. The thermal profile is illustrated in the figure below.

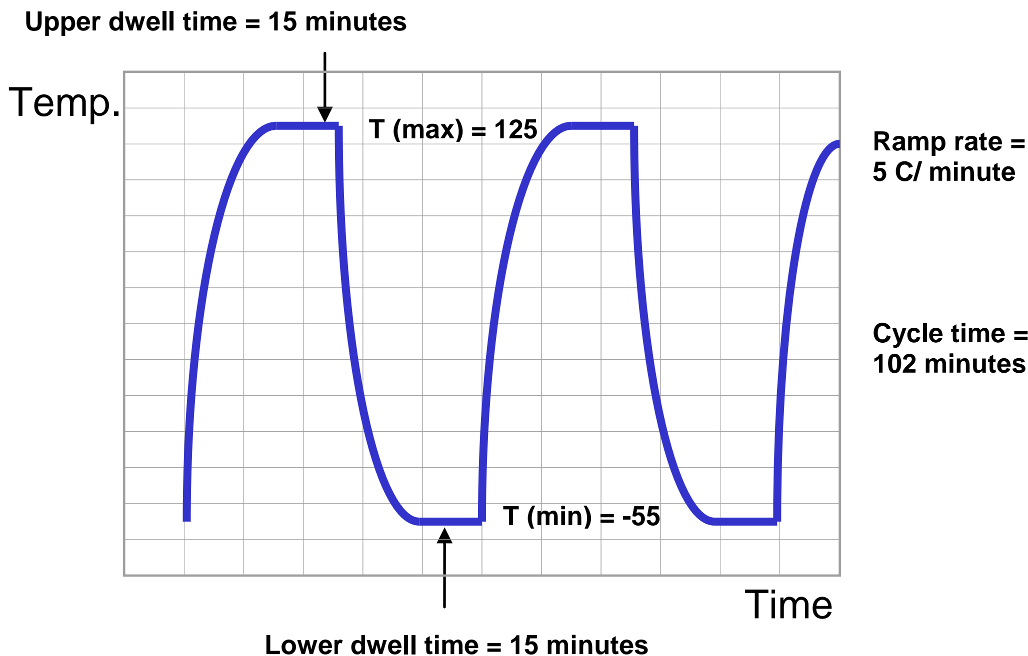

Figure 3: Thermal Cycling Temperature Profile

The following figure shows the data logger connections to the test vehicles during thermal cycling at the Textron Systems facility.

Figure 4: Data Logger and Test Vehicles

Results and Discussion

Rework

Upon review of the main effects plot, it can be seen that the SAC 305 solder had a much lower mean contact time of 65.1 s as compared to 87.9 s for tin/copper solder. Process #1 had a much lower mean contact time of 67.8 s as compared to the mean contact time of 139.4 s for Process #2. The only difference between these two processes was the type of nozzle used. Process #1 used the standard nozzle and Process #2 used the hybrid nozzle. The contact time required for solder flow through to the topside of the rework coupon was much greater for the hybrid nozzle than for the standard nozzle. Process #3 had the lowest mean contact time of 31.6 s because there was no contact time during the component removal process when using the Air Vac machine.

The mean contact time for the ENIG (71.7 s), nano (69.8 s), and HASL (76.7 s) surface finishes were all between 69 to 77 s. The contact time for the OSP surface finish was the highest of the four surface finishes with a mean time of 88.7 s. The figure below show the main effects plot for contact time.

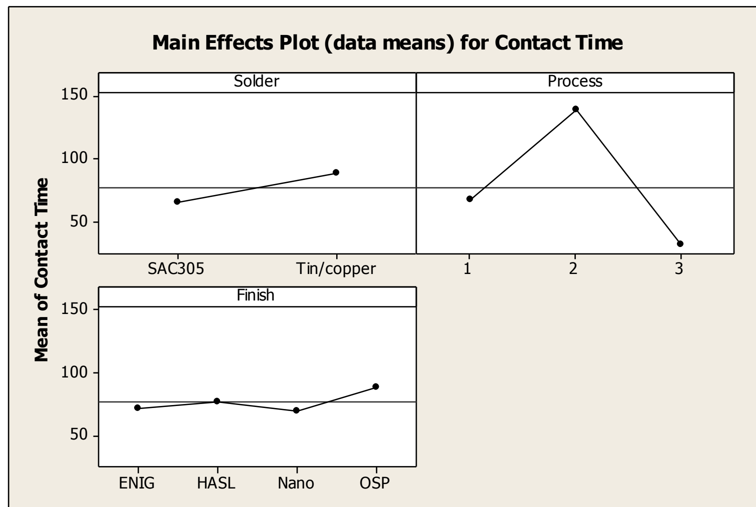

Figure 5: Main Effects Plot for Contact Time

Copper thickness measurements were taken at three different locations: 1) bottom side knee, 2) topside pad, and 3) topside barrel wall. The bottom side knee location is most susceptible to copper dissolution due to its geometry and close vicinity to the solder in the nozzle during the rework process.

Since there was significant variation of copper thickness between the different rework coupons, the following calculation was used to determine the average copper thickness for each rework coupon.

- Avg. copper thickness = (topside pad thickness + topside barrel thickness) / 2 (1)

Once the average copper thickness was determined, then the following formula was used to calculate the copper dissolution for each of the rework coupons.

- Copper dissolution = average copper thickness – knee thickness (2)

The copper thickness at the bottom side knee location was considered to be the minimum thickness of the copper for the rework coupon. The bottom side knee copper thickness was compared to IPC 6012B "Qualification and Performance Specification for Rigid Printed Boards" standards for minimum copper thickness (IPC 2004). The target level for the rework efforts was to achieve a Class 3 level which is a minimum of 1.0 mil copper thickness. The IPC 6012B standards for minimum copper thickness are provided below.

- Class 3: minimum of 0.001" copper (1.0 mil)
- Class 2: minimum of 0.0008" copper (0.8 mils)
- Class 1: minimum of 0.0006" copper (0.6 mils)

The following figure shows the Main Effects Plot for copper dissolution after completion of a single rework.

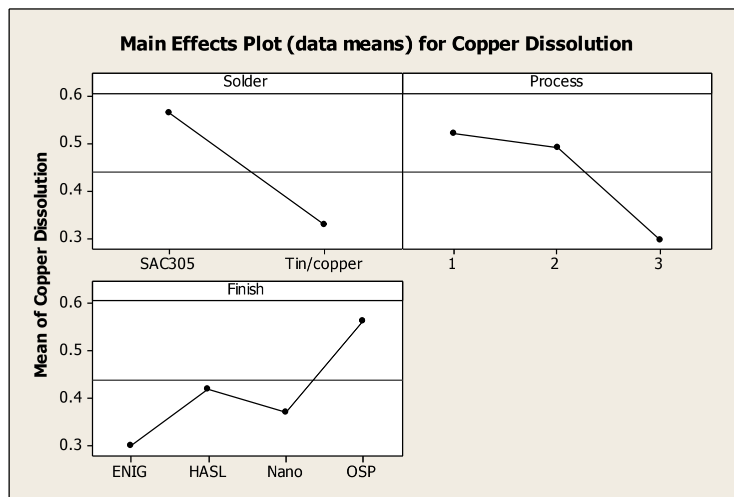

Figure 6: Main Effects Plot for Copper Dissolution

Upon review of the Main Effects Plot for copper dissolution, the following results were obtained.

- Tin/copper solder had 42% less copper dissolution than SAC305 solder.
- The hybrid nozzle used in Process 2 had 6% less copper dissolution than the standard nozzle used in Process 1.
- Use of the Air Vac for component removal (Process 3) provided 43% less copper dissolution than Process 1.
- ENIG had the lowest copper dissolution, and the nano surface finish had the least amount of copper dissolution for a surface finish without a nickel barrier.

Thermal Cycling

For the purposes of analyzing the results of the thermal cycling data, a minimum of 63% of failures is preferred in order to plot the Weibull distribution. Therefore, the Weibull distribution was only provided for the component types that have achieved a minimum of 63% failures during thermal cycling at the time that this report is finalized. Once the Weibull plot is generated for a component type, and then various points of interest can be calculated such as the number of cycles to 1% cumulative failure (N_1), number of cycles to 50% cumulative failure (N_{50}), or characteristic life (N_{63})

From this distribution, acceleration factors are used to convert life expectancies in the thermal chamber test environment to life expectancies for normal use environments or field conditions. There are several models developed for predicting the fatigue life of solder joints. These models are based on one or more of the fundamental mechanisms that can cause solder joint damage. These fundamental mechanisms include plastic strain based, creep strain based, energy based, and damage accumulation based.

The Norris-Landzberg model was selected because it is a sophisticated model that takes into account the effects of creep and stress relaxation. The model also takes into account the cyclic frequencies and the temperature dependent properties of solder. The Norris-Landzberg model can be used for predicting the fatigue life of both tin/lead and lead-free solder joints. This model requires that the test vehicle and the product in field operations have the same material properties and design parameters. (Engelmaier 2002) The formula for the acceleration factor (AF) using this model is as follows (Norris, 1969, Shina, 2008):

$$AF = N_O / N_t \quad (3)$$

$$AF = (\text{delta } T_t / \text{delta } T_O)^B * (t_t / t_O)^Y * \exp\{(E_a/k * (1 / T_{max,O} - 1/T_{max,t})\} \quad (4)$$

Where AF = Acceleration Factor

N_O = Number of cycles to failure (operation conditions)
N_t = Number of cycles to failure (test conditions)
T_t = Temperature (test conditions)
T_O = Temperature (operation conditions)
B, Y = fitting parameters
t_t = Time duration of thermal cycle (test conditions)
t_O = Time duration of thermal cycle (operation conditions)
k = Boltzman's constant
E_a = Activation energy
$T_{max,O}$ = Maximum temperature (operation conditions)
$T_{max,t}$ = Maximum temperature (test conditions)

The first term in the Norris-Landzberg equation accounts for the effect of the temperature range for both the test and operation conditions. The second term in the Norris-Landzberg equation accounts for the effect of temperature range. The third term in the Norris-Landzberg equation accounts for the effect of the maximum temperature.

The values for B, Y, and Ea/k for tin/lead solders in the Norris-Landzberg model are well studied and available in literature. In 2006, Pan et al. conducted research to develop values for B, Y, and Ea/k in the Norris-Landzberg model for SAC solder joints for three different surface mount component package styles: ceramic ball grid arrays (CBGA), chip scale package (CSP), and thin small outline package (TSOP). The B, Y, and Ea/k values used for tin/lead solders and the values developed by Pan et. al for SAC solder are provided in the table below (Pan, 2006). These values were used for determining the acceleration factor for both the tin/lead and SAC solder pastes used for this research.

Table 7: Norris-Landzberg Exponents

Parameter	Tin/Lead Solder	Lead-free (SAC) Solder
B	1.9	2.65
Y	0.33	0.136
Ea/k	1,414	2,185

The two test vehicles with halogen-free laminate material had early failures for all components. The components on the two test vehicles with halogen-free laminate material had all failed by 220 thermal cycles. A summary of the thermal cycling failure data for the sixteen test vehicles in the DOE is provided in the table below for the daisy chains connected to only one component.

Table 8: Thermal Cycling Data for Daisy Chains with One Component

Comp-onent RefDes	Component Type	Number of Failures	Number of Daisy Chains	Percent Failed
U16	Chip array BGA, 100 balls (1.0 mm pitch)	12	16	75.0%
U17	Tape array microBGA, 64 balls (0.5 mm pitch)	9	16	56.3%
U26	Ceramic microBGA, 84 balls (0.5 mm pitch)	8	16	50.0%
U1, U2, U24, U25	TSOP, 48 Pins	13	56	23.2%
U15	PQFP, 208 pins	1	16	6.3%
U14, U18	Plastic BGA, 256 balls (1.0 mm pitch)	1	32	3.1%

The component located at reference designator U16 was the first component to surpass the 63% threshold. To date, twelve out of the sixteen test vehicles from the Design of Experiments had failures with the U16 component. This resulted in a 75.0% failure rate that exceeds the 63% threshold. Therefore, the Weibull distribution, acceleration factor, and operational life estimates were generated for this component. A summary of the thermal cycling failure data after 1,470 thermal cycles is provided in the table below for the daisy chains connected to more than one component.

Table 9: Thermal Cycling Data for Daisy Chains with More Than One Component

Component Type	Quantity of Components per Daisy Chain	Number of First Failures	Number of Daisy Chains	Percent of Daisy Chains with First Failure
0805 Resistor	49 - 52	23	32	71.9%
0402 Resistor	100	8	16	50.0%
0603 Resistor	100	7	16	43.8%

The three different resistors (0805, 0603, and 0402) are industry standard packages. These components had the same component finish and were made by the same manufacturer. The primary difference between the resistors is physical size. The 0805 resistor is the largest, and the 0402 resistor is the smallest. The 0805 resistor had the highest percentage (71.0%) of daisy chains where the first failure was identified.

The U16 component is a surface mount component that is a ball grid array. The component has 100 balls, a 1.0 millimeter pitch, and an 11 millimeter body size. The ball matrix size is 10 millimeters by 10 millimeters. For components assembled on the tin/lead test vehicles, the solder ball material is eutectic tin lead solder. For the components assembled on the lead-free test vehicles, the solder ball material is SAC solder. The package thickness is 1.5 millimeters, and the package material is bismaleimide-triazine. (Practical, 2007)

Weibull probability plots were used to model the failure data obtained during the thermal cycling testing. The two parameter Weibull distribution is defined by the following two parameters: shape and scale. The shape parameter describes the shape of the Weibull curve. A shape value of "3" approximates a normal curve. A shape value between "2" and "4" is still somewhat normal. A shape value lower than two low describes a right-skewed curve, and a shape value greater than four describes a left-skewed curve. The scale parameter is the 63.2 percentile ($N_{63.2}$) of the data. The scale parameter is sometimes referred to as characteristic life. The Weibull probability density function used by Minitab is as follows. (Minitab, 2008)

$$F(x) = \{ax^{a-1} * e^{-(x/b)a}\} / ba, x>0 \quad (5)$$

Eight out of the twelve lead-free test vehicles have experienced failures for the U16 component. The shape parameter calculated for U16 on lead-free test vehicles is 0.54, and the scale parameter calculated for U16 on lead-free test vehicles is 932.7. The following figure shows the Weibull distribution for the U16 component on lead-free test vehicles.

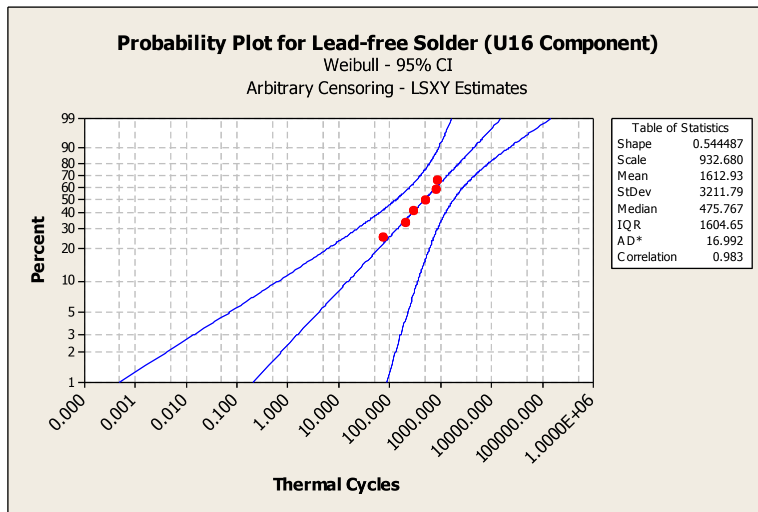

Figure 7: Weibull Distribution for the U16 Component on Lead-free Test Vehicles

All of the four tin/lead test vehicles have experienced failures for the U16 component. The shape parameter calculated for U16 on tin/lead test vehicles is 1.06, and the scale parameter calculated for U16 on tin/lead test vehicles is 718.3. The following figure shows the Weibull distribution for the U16 component on tin/lead test vehicles.

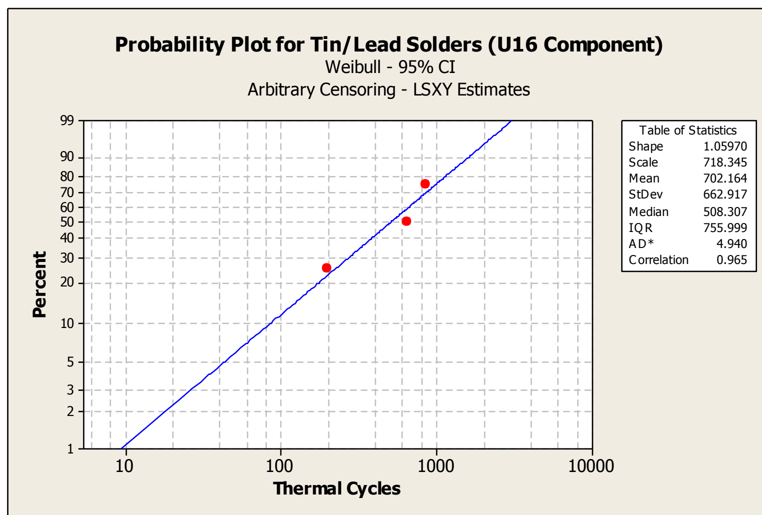

Figure 8: Weibull Distribution for the U16 Component on Tin/Lead Test Vehicles

The Weibull distribution is used to determine the percent of test vehicles that are anticipated to fail by a particular time under test conditions. The Table of Percentiles provided by Minitab for both the lead-free and tin/lead test vehicles for the U16 component is provided in the table below.

Table 10: Table of Percentiles for U16 Component

Percent	Designation	Lead-free Percentile	Tin/lead Percentile
1	N_1	0.2	9.4
10	N_{10}	15.0	85.9
20	N_{20}	59.3	174.4
30	N_{30}	140.4	271.5
40	N_{40}	271.6	381.1
50	N_{50}	475.8	508.3
60	N_{60}	794.3	661.5
63.2	$N_{63.2}$ (scale value)	932.7	718.3
70	N_{70}	1,311.6	855.9
80	N_{80}	2,235.2	1,125.6
90	N_{90}	4,314.9	1,578.1

For the component U16, the tin/lead test vehicles appear more robust from N_1 through N_{50}. However, there is a crossover point after N_{50}, and from N_{60} through N_{90} the lead-free test vehicles appear more robust. This indicates that there may be two different failure modes involved, one is possibly an infant mortality related failure mode and the other is possibly a wear out mechanism failure mode. (O'Connor, 2002) There is further evidence for this situation because there are four lead-free test vehicles that have not had failures for the U16 component; however, there have been U16 failures to date for all four of the tin/lead test vehicles.

After the failure data for component U16 had been characterized for thermal cycling conditions, it was necessary to extrapolate the reliability performance from test conditions to actual operation conditions. Three actual operation conditions with reliability implications were chosen that are relevant to members of the New England Lead-free Electronics Consortium. These conditions include small business IT systems, automotive and aerospace operation conditions. The minimum and maximum temperatures, as well as the cycle time frequency for these operation conditions are provided in the table below.

Table 11: Test and Operation Conditions

Application	Minimum Temp.	Maximum Temp.	Temp. Cycles per Day	Temp Cycle Duration
Thermal Cycling (Test)	- 55 °C	+ 125 °C	14.1	102 minutes
Aerospace	- 40 °C	+ 125 °C	14 - 16	90 – 102.8 minutes
Automotive	- 40 °C	+ 85 °C	2 - 5	288 – 720 minutes
Small Business IT Systems	+ 10 °C	+ 70 °C	2	720 minutes

The Norris-Landzberg model was used to calculate the acceleration factor for each of the three operation conditions above. The higher end of the range of the temperature cycles per day were used for the aerospace and automotive applications. The acceleration factors calculated are as follows:

Aerospace: 1.1
Automotive: 4.2
Data Center: 27.2

The acceleration factor was then applied to the N_x expected life during test conditions to calculate the N_x for actual product life for various applications. The anticipated product life for lead-free test vehicles in aerospace, automotive, and small business IT systems applications are provided in the table below.

Table 12: Product life For Lead-free Solders

Application	Acceleration Factor	N_{10} Test Cycles	N_{10} Operation Cycles	$N_{63.2}$ Test Cycles	N_{50} Operation Cycles
Aerospace	1.2	15	18	933	1,120
Automotive	5.6	15	84	933	5,225
Small Business IT Systems	57.8	15	867	933	53,927

The anticipated product life for tin/lead test vehicles in aerospace, automotive, and small business IT systems applications are provided in the table below.

Table 13: Product Life For Tin/lead Solders

Application	Acceleration Factor	N_{10} Test Cycles	N_{10} Operation Cycles	$N_{63.2}$ Test Cycles	N_{50} Operation Cycles
Aerospace	1.1	86	95	718	790
Automotive	4.2	86	361	718	3,016
Small Business IT Systems	27.2	86	2,339	718	19,530

For the U16 component at N_{10} cycles, it can be seen that the operation cycles is much higher for all applications for the test vehicles that are made with the tin/lead solder as compared to the test vehicles made with lead-free solder. For example, the N_{10} operation cycles for the automobile application using lead-free solder is 86 cycles, while the operation cycles for tin/lead solder is 361 cycles. The converse situation is true for N_{50} cycles.

Nineteen out of the twenty-four lead-free daisy chains with the 0805 component have experienced failures. The shape parameter calculated for 0805 on lead-free test vehicles is 5.3, and the scale parameter calculated for 0805 on lead-free test vehicles is 886.8. The following figure shows the Weibull distribution for the 0805 component on lead-free test vehicles.

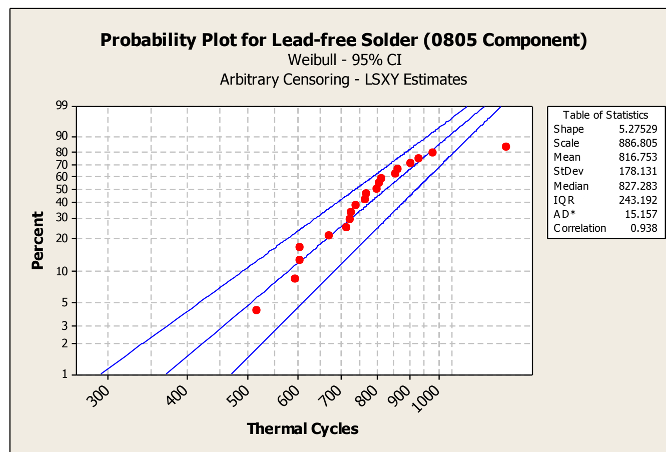

Figure 9: Weibull Distribution for the First Failure of the 0805 on LF Test Vehicles

Four out of the eight tin/lead daisy chains with the 0805 components have experienced failures. The shape parameter calculated for 0805 on tin/lead test vehicles is 2.4, and the scale parameter calculated for 0805 on tin/lead test vehicles is 1,660.7. The following figure shows the Weibull distribution for the 0805 component on tin/lead test vehicles.

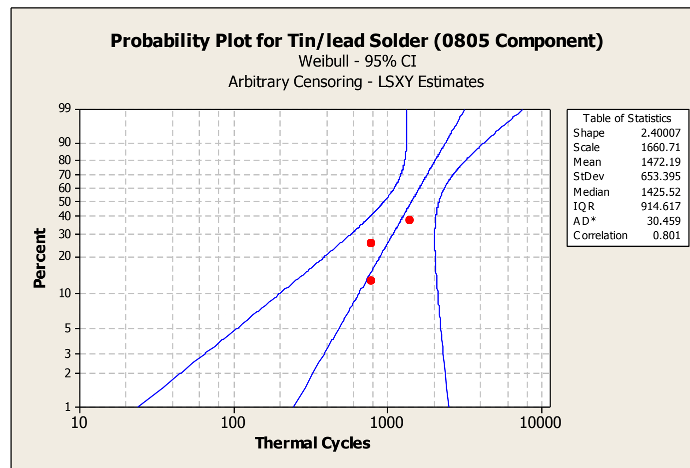

Figure 10: Weibull Distribution for the First Failure of the 0805 on TL Test Vehicles

The Table of Percentiles provided by Minitab for both the lead-free and tin/lead test vehicles for the 0805 component is provided in the table below.

Table 14: Table of Percentiles for 0805 Component

Percent	Designation	Lead-free Percentile	Tin/lead Percentile
1	N_1	370.8	244.3
10	N_{10}	578.8	650.3
20	N_{20}	667.3	889.0
30	N_{30}	729.4	1,080.8
40	N_{40}	780.8	1,255.3
50	N_{50}	827.3	1,425.5
60	N_{60}	872.2	1,601.3
63.2	$N_{63.2}$ (scale value)	886.8	1,660.7
70	N_{70}	918.6	1,794.3
80	N_{80}	970.5	2,024.9
90	N_{90}	1,038.7	2,350.8

For the 0805 component, the lead-free test vehicles appear more robust than the tin/lead test vehicles for the N_1 percentile. However, there is a crossover point after N_1, and from N_{10} through N_{90} the tin/lead test vehicles appear more robust.

This indicates that there may be two different failure modes involved, one is possibly an infant mortality related failure mode and the other is possibly a wear out mechanism failure mode.

Conclusions

The rework coupons that used the tin/copper solder had greater contact time, but less copper dissolution than the coupons using the SAC305 solder for the single rework efforts. Therefore, the type of solder alloy was a greater contributing factor to copper dissolution than the contact time for this research. The rework coupons that used Process 2 (hybrid nozzle) had greater contact time but less copper dissolution than Process 1 (standard nozzle). Therefore, the hybrid nozzle was effective at reducing the copper dissolution even though it required additional contact time.

The rework coupons that used Process 3 had less contact time and less copper dissolution than both Process 1 and Process 2. The reduction in contact time is attributed to the use of the Air Vac equipment for the component removal. The rework coupons with the ENIG surface finish had the lowest copper dissolution because of the protective nickel barrier. The rework coupons with the nano surface finish had the least amount of copper dissolution for a surface finish without a nickel barrier. Finally, there were no signs of thermal degradation to the laminate or the components during rework efforts. Therefore, successful rework efforts are possible with lead-free materials that can achieve Class 3 standards without signs of thermal degradation.

Thermal cycling is ongoing, having completed 1,470 cycles. The following preliminary conclusions were made during this research.

- Halogen free test vehicles had early failures for all components. Further development is needed in halogen free laminate technology before it is viable as a bromide replacement for fire retardant functions.
- Test vehicles with High Tg FR4 laminate material are robust with only 2 component types (BGA and 0805 resistor) surpassing 63% failure threshold after 1,470 cycles of severe thermal conditions.
- The results for the BGA component (U16) showed that tin lead is more reliable than lead-free for early failures, but less reliable for wear out failures. This is a crossover mechanism that indicates multiple failure modes.
- Resistor 0805 resistor showed reverse reliability properties than the U16 BGA.

In conclusion, there is inadequate data collected to date in order to fully evaluate tin lead versus lead free reliability for the research test vehicle. This inadequate data will be addressed in the further study section.

Further Study

The consortium plans to complete the reliability testing and the subsequent failure analysis in 2009. The plan is to finish the Phase IV project by the end of the grant period in September 2009. This additional research will include the following:

- Complete thermal cycling until 63% failure threshold has been achieved for components on all daisy chain circuits.
- Conduct vibration testing on test vehicles
- Perform failure analysis of failed components to determine actual failure modes.

Acknowledgements

The authors would like to acknowledge the contributions from the following individuals and corporations for their support of this research: Freedom CAD for design of the test vehicle, DDI for providing the test vehicles, Texas Instruments for providing components, AIM for providing solder for assembly of through hole components, Isola for providing laminate materials for the test vehicles, Ormecon for providing the nano surface finish, George Wilkish, Prime Consultant for participation in consortium and design subgroup meetings, International Rectifier for providing components, Stentech for providing stencils, and PWB Interconnect Solutions for IST testing. In addition, the authors wish to acknowledge the EPA Region 1 for providing two grants for funding for this project during the period 2006 – 2009 (Award Nos. NP 971586010 and X9-97182701-0).

References

Engelmaier, Werner, Solder Joint Reliability – Part 3: Comparing Different Solder Fatigue Models, Global SMT & Packaging, pp. 35 – 36, August, 2002.

Farrell, Robert, Paul Bodmer, Bruce Tostevin, Richard Russo and Gregory Morose, “Pb-free PTH Rework on a Thick, Heavy Assembly”, Circuits Assembly Magazine, pp. 2 – 6, August 2007.

Farrell, Robert, Russo, Richard, Morose, Gregory, Mazur, Scott, “Transition to Lead-free Electronics Assembly Case Study Part II: Product Reliability and Forced Rework”, Submitted for IPC/JEDEC Global Conference on Lead free Reliability and Reliability Testing, Boston, pp. 2 – 5, April 2007.

IPC, IPC 6012B “Qualification and Performance Specification for Rigid Printed Boards”, pp. 4 – 22, August 2004.

IPC-9701 Standard “Performance Test Methods and Qualification Requirements for Surface Mount Solder Attachments”, IPC Association Connecting Electronics Industries, pp. 1-3 through 1-6, January 2002.

Manock, John, et al., Effect of Temperature Cycling Parameters on the Solder Joint Reliability of a Pb-free PBGA Package, SMTA Journal, Volume 21 Issue 3, pp. 36 – 45, 2008.

Minitab, Interpreting the Shape, Scale, and Threshold on a Weibull Probability Plot, www.minitab.com/support/answers, August 2008.

Norris, K. C., Landzberg, A. H., Reliability of Controlled Collapse Interconnections, IBM Journal of Research and Development, pp. 266-271, May 1969.

O’Connor, Patrick D. T., Practical Reliability Engineering, Fourth Edition, John Wiley & Sons Ltd, West Sussex, England, pp. 4 – 20, 2002.

Pan, N., An Acceleration Model for Sn-Ag-Cu Solder Joint reliability Under Various Thermal Cycle Conditions, SMTAI, pp. 876-883, 2006.

Practical Components, Product Catalogue - Chip Array Ball Grid Array, pp. 12 – 14, 2007.

Shina Sammy G., “Six Sigma for Electronics Design and Manufacturing”, McGraw Hill, New York, April 2002.

Shina, Sammy G., Green Electronics Design and Manufacturing – Reliability of Green Electronic Systems, McGraw-Hill, New York, pp. 177 – 246, 2008.